Microscopic theory for quantum evaporation from a superfluid surface

P. A. Mulheran and J. C. Inkson
Department of Physics, University of Exeter, Stocker Road, Exeter, United Kingdom
(Received 24 February 1992)

Beliaev's microscopic theory of superfluidity in ^{4}He is applied to an inhomogeneous system with a free surface. The equations of motion are analyzed within a local-density approximation and a set of WKB solutions are found. Perturbation theory is used to provide the mixing between these states. The probabilities for evaporation, reflection, and adsorption from the surface are calculated for excitations in the system. The probabilities for the evaporation of phonons and rotons are in reasonable agreement with experiment. We find that low-energy incident atoms tend to condense as phonons and high-energy atoms condense as R^+ rotons. These results are again in qualitative agreement with experiment, provided that the short lifetimes of phonons with energies < 10 K are accounted for.

I. INTRODUCTION

Since its discovery,[1] the superfluidity of ^{4}He has been a topic of considerable interest, largely because of the fact that it is an ideal system on which to test the fundamental concepts of quantum mechanics. One of the principal notions of a many-body system in the quantum regime is that of Landau's quasiparticles,[2] which holds that the excited states of the fluid should exhibit particlelike properties. That this is the case has long been established by neutron-scattering experiments.[3] The interaction between these quasiparticles and the free surface of a superfluid sample, giving rise to the evaporation of atoms into the vapor, has recently been investigated in a number of experiments.[4–9] These experiments have been developed to such a degree that they now provide a good means of probing the nature of the quasiparticles[10] and how they interact with one another. Despite the progress made experimentally, a satisfactory microscopic theory for the evaporation process has not yet been given. The aim of this work is to provide such an analysis and to predict the probabilities of various scattering events at the surface.

Evaporation from the superfluid state became of interest with the experiments of Johnston and King,[4] who studied the energy distribution of atoms in the vapor above a thermal bath of superfluid held at 0.6 K. The results were interpreted as showing that the evaporated atoms had a characteristic temperature of 1.6 K, 1 K higher than the fluid. An explanation for this was subsequently given by Anderson[11] and Hyman, Scully, and Widom.[12] These authors conjectured that the evaporation occurred by the conversion of quasiparticles at the free surface to atoms in the vapor, essentially as a one-to-one process, since these transitions have larger phase spaces than those involving more than one final state. The quasiparticles primarily responsible would be rotons, which have a high density of states, so that the kinetic energy given to the atoms would be about 8.8 K$-\mu$, where μ is the binding energy of the atoms to the liquid (see Fig. 1). This chemical potential μ is 7.16 K, so that most of the liberated atoms would have an energy of $\sim$1.6 K, in agreement with the reported experimental results. It later emerged[13] that Johnston and King were mistaken in their conclusions; their results were seriously affected by interatomic scattering in the vapor. Furthermore, Cole[14] pointed out that the rotons with a high density of states necessarily have low group velocities, so that the flux of these rotons, from a thermal bath, into the surface would be no larger than that of the other excitations. Thus the theoretical explanations for the results were also in error. Nevertheless, the phase-space arguments of Anderson[11] still remain an important contribution to the understanding of the processes involved and the concept of quantum evaporation has survived.

The investigation of this phenomenon was continued

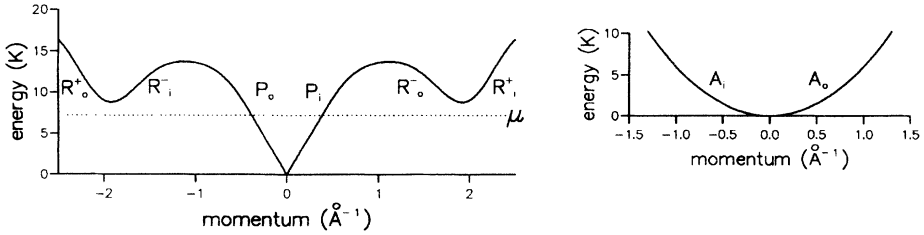

FIG. 1. Bulk quasiparticle spectrum with the free-atom spectrum alongside. The zero energy of the atomic spectrum is equal to the chemical potential μ of the bulk liquid. The various branches of the curves are labeled by type with the suffix indicating the direction of travel (either into or out of the surface).

by Balibar *et al.*[5] and Baird, Hope, and Wyatt.[6] Instead of using samples in thermal equilibrium, which of necessity involve averaging over all the quasiparticle-energy range, these authors used collimated beams of quasiparticles to test the evaporation mechanism. These beams were generated by minute heat pulses given to metal films suspended in the liquid just below the surface. In the vapor above superconducting, bolometers detected the arrival of evaporated atoms and the time of flight of the signals confirmed the one-to-one conjecture of the quasiparticle to atom transition. In addition to this, Brown and Wyatt[8] have used a diffraction effect to distinguish between the rotons and phonons. Because of the purity of the system, the liquid with a free surface has translational symmetry along the interface, which then requires that the component of momentum parallel to the surface be conserved in any quasiparticle-scattering process. Since phonons and rotons with the same energy have in general very different momenta, the evaporated atoms emerge in different directions depending upon the type of quasiparticle causing its release. Brown and Wyatt have found the expected signals due to phonons and positive-group velocity rotons (R^+), but not those due to the negative-group-velocity rotons (R^-). This feature is attributed to the failure of the heater to produce such R^- rotons; however, R^- excitations have been produced by condensing atoms[9] in an experiment that also utilizes the diffraction effect. Computer modeling of the measured signals as a function of time and angle has shown that the evaporation is very probably a one-to-one process and that parallel momentum is indeed conserved in the transition. Also, since higher-order processes involving the transmission of an atom *plus* the reflection of a secondary phonon or ripplon will cause the transmitted signal to broadening in its angular spread, the authors of Ref. 8 have been able to place an upper limit of 1 K on the energies of these secondary reflections. It therefore appears that Anderson's phase-space restriction[11] on these secondary processes is working in practice and that we should concentrate our efforts on the understanding of the one-to-one (quantum) evaporation process.

One of the difficulties with the above experiments is in the calibration of the detectors; for various reasons, it is difficult for the experimentalists to deduce absolute values for the probabilities of quasiparticle evaporation. This makes theoretical predictions even more important. There is, however, one relevant experiment that has been well calibrated; this measures the probability of reflection for atoms impinging upon the surface. Edwards *et al.*[15] reported that the reflection probability for most atoms is extremely low, typically between 10^{-3} and 10^{-2}. This probability rises to unity for low-energy atoms and for atoms incident at glancing angles. They also reported that the reflections are almost entirely specular (less than 10^{-3} scatter diffusely) and that the data shows very little structure. This implies that the reflectivity is independent of the form of the quasiparticle spectrum in the liquid, and they proposed that the reflections were due largely to the weak van der Waals interaction between liquid and atoms. Any atoms that come too close to the surface are then completely absorbed by the liquid, although Edwards *et al.* were unable to say exactly how these atoms give their energy to the liquid. Subsequently, Echenique and Pendry[16] proposed that the absorbed energy was dispersed in a shower of surface-tension waves (ripplons); their calculations showed that before any atoms were able to penetrate the surface region they would have lost the majority of their energy to ripplons and hence could not create any bulk quasiparticles apart from low-energy phonons. In this manner Echenique and Pendry predicted a reflectivity curve close to the experimental results. However, we should note that, since this work, experimental results have emerged that contradict this theory. First, Edwards, Ihas, and Tam[17] have measured bulk quasiparticle signals produced by a condensing beam of atoms, and they reported that one-to-one conversion of atoms to quasiparticles cannot be ruled out with their low-efficiency detector. Second, Wyborn and Wyatt[18] have analyzed their results for the production and detection of R^- rotons and can place a lower limit of 0.25 on the probability of an atom condensing as a roton in their particular experiment. Finally, we note that the strong evaporation signals observed experimentally also suggest that the ripplons are having small effect on the trajectory of atoms. Therefore we cannot regard the reflectivity results as being satisfactorily explained, and so we are justified in considering the atom-reflectivity and quantum-evaporation processes as two halves of the same problem: That is how the liquid quasiparticles and vapor atoms couple at the surface.

We now consider the general types of process that are possible in the scattering of the particles from the surface. The boundary conditions are that energy and parallel momentum are conserved in the process and that only the one-to-one conversions are significant. Ripplons will be completely neglected, and we will assume that all of the quasiparticle states are stable and able to propagate ballisticly (this is not true for phonons below 10 K, which can decay via the three-phonon process[19]). Figure 2(a) shows the possible outgoing states for an incident atom (refer to Fig. 1 for the particle labels). There are three different transmitted quasiparticles and one reflected atom to be considered. Figures 2(b)–2(d) illustrate the possible transitions involved in the evaporation processes where there is one transmitted mode and three reflections. In particular, the quasiparticle reflections include the possibility of mode changing; this has recently been observed by Wyborn and Wyatt.[18] In all of these cases, there exists the possibility of evanescent modes if the incident excitation carries too much parallel momentum for an outgoing mode of the same energy to support, as is usual in diffraction phenomena. For transmission to be possible, the quasiparticles must have energy above the chemical potential of 7.16 K, and from Fig. 1 it can be seen that there are essentially three energy ranges of interest. First, incident atoms with energy less than 1.6 K can only couple to bulk phonons. Second, when the excitation energy is between that of the roton minimum and phonon maximum (maxon), all three bulk-liquid modes will be involved. Third, the high-energy atoms can only couple to the high-energy R^+ rotons.

Previous discussions of the transitions outlined above

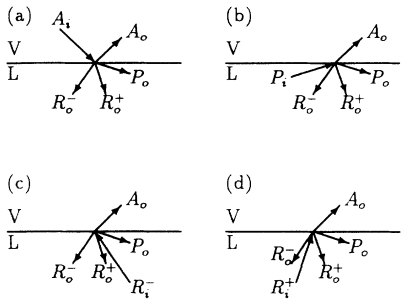

FIG. 2. Possible emissions from incident excitations: (a) incident atoms, (b) incident phonons, (c) incident R^- rotons, and (d) incident R^+ rotons.

have centered on the use of a tunneling Hamiltonian formalism.[12,14,21] However, it is clear that in the current problem, where the coupling between the atoms and quasiparticles is strong,[15] this approach is inadequate. Further, since the liquid and vapor comprise the same material, it seems that the distinction between liquid and vapor operators made in the tunneling approach is inappropriate. In this work we have applied the microscopic superfluid theory of Beliaev[22] to the problem. In Sec. II we review this theory and show how it can give an equation of motion for the quasiparticles in an inhomogeneous system. The liquid surface is then described in terms of a density variation. The equations are solved in the local-density approximation and WKB solutions derived. To find the couplings between these solutions, first-order perturbation theory is used with the full nonlocal potential. The resulting expressions for the probabilities are evaluated using the experimentally measured excitation spectrum and the results of the calculations presented in Sec. III. We have restricted ourselves at this stage to the case of normally incident particles because of numerical difficulties in the evaluation of the probabilities for nonzero parallel-momentum scatterings. Finally, we compare the results of this work with the experimental evidence and discuss the implications in Sec. IV.

II. APPLICATION OF BALIAEV'S THEORY TO QUANTUM EVAPORATION

A. Theory of bulk He II

The fundamental idea behind most theories of superfluidity is that of Bose condensation. That this is associated with the λ transition observed in liquid ^{4}He was proposed by Tisza,[23] and recent experiments suggest that the condensate fraction in the superfluid is $\sim 10\%$.[24] Bogoliubov used this macroscopic occupation of the zero-momentum atomic orbital to deduce the quasiparticle spectrum.[25] He showed that the Hamiltonian for the liquid can be diagonalized to leading order in the condensate density by a linear canonical transformation. The excited states of the system are then noninteracting boson particles, which have specific momentum $\hbar k$ and energy $E(k)$. These quasiparticles are many-body states involving extra occupation of both the $+k$ and the $-k$ atomic orbitals. The Bogoliubov energy spectrum is

$$E(k)=\left[\left[\frac{\hbar^2k^2}{2m}\right]^2+2\rho_0V_k\frac{\hbar^2k^2}{2m}\right]^{1/2}, \tag{1}$$

where m is the atomic mass, ρ_0 is the condensate density, and V_k is the momentum-dependent scattering amplitude between two atoms. Brueckner and Sawada[26] have shown that this formula gives quite a good fit to the experimentally observed spectrum if V_k is a $x^{-1}\sin x$ function. They interpret this as the s-wave-scattering matrix for two hard spheres of radius 2.26 Å, which is close to the radius of real helium atoms ($\sim$2.25 Å). For our purposes the Fourier transform of V_k furnishes us with a spatial pseudopotential $V(r)$ for the interatomic interaction which will be used in this study.

Beliaev's theory for the bulk superfluid[22] uses many-body Green's-function techniques to calculate the quasiparticle properties of the system. It is most easily understood in the context of the Bogoliubov theory, and we shall be using his approximations for the Hamiltonian. We have that ground state of the interacting system is the condensate plus the depletion effect which results in the occupation of finite-momentum atomic orbitals. Hence the action of an annihilation operator upon the ground state is generally nonzero and we must consider the effect of scattering events that are not present in many normal systems. Using Bogoliubov's assumption that the excited states are dominated by scatterings involving two condensate particles, Beliaev found three distinct self-energies. These are illustrated in Fig. 3(a), where the dotted lines represent the creation (or annihilation) of condensate particles. These are to be inserted into the Feynman diagrams for the quasiparticle propagator in such a

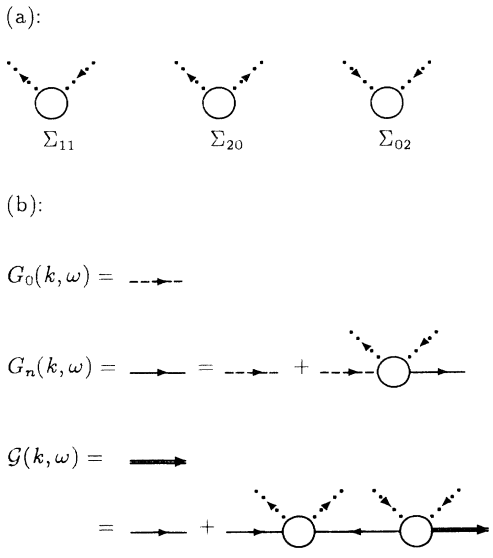

FIG. 3. (a) Three self-energies: Σ_{11} has one particle entering the condensate and one leaving, Σ_{20} has two entering, and Σ_{02} has two leaving the condensate. (b) The coupled Dyson equations for the propagators of the system. G_0 is the free-particle propagator, G_n is the propagator for a "normal" system, and $\mathcal{G}$ is the quasiparticle propagator for the superfluid system.

way that the number of particles is conserved throughout. Beliaev then found the algebraic (Dyson) equations for the propagator [Fig. 3(b)]. Taking the same low-density limit as Bogoliubov, Beliaev approximated the self-energies as

$$\Sigma_{11}=\rho_0 V_0+\rho_0 V_k,\quad \Sigma_{20}=\Sigma_{02}=\rho_0 V_k\ . \tag{2}$$

Hence he found the quasiparticle Green's function $\mathcal{G}(k,\omega)$, the poles of which gave the energy spectrum to be the same as that of Bogoliubov [Eq. (1)].

B. Local-density approximation for inhomogeneous systems

We start our description of a system with a free surface by allowing the condensate density ρ_0 to vary with position. Deep in the liquid, it has the value of the bulk superfluid condensate and the Beliaev Green's function describes the quasiparticle states. High above the surface region, the condensate density is zero. In this case the energy spectrum (1) is just that for noninteracting atoms and Beliaev's propagator describes free atoms. We see that Beliaev's theory will be valid also for any constant value of the density in between these extremes. To make use of this, we require a real-space equation of motion for the quasiparticles. By rearranging the equations shown in Fig. 3(b), we find

$$[G_0^{-1}(k,\omega)-\Sigma_{11}(k,\omega) -\Sigma_{20}(k,\omega)G_n(-k,-\omega)\Sigma_{02}(k,\omega)]\mathcal{G}(k,\omega)=1\ . \tag{3}$$

The Fourier transform of this equation gives the equivalent real-space equation of motion for the Green's functions and hence the quasiparticle wave functions

$$\left[\omega-\mu+\frac{\hbar^2\nabla^2}{2m}\right]\varphi(r_1)-\int\Sigma(r_1,r_3,\omega)\varphi(r_3)d^3r_3=0\ . \tag{4}$$

Here the first term is the total energy of the quasiparticle with respect to the chemical potential μ minus the kinetic energy, while the second is the potential-energy term. The self-energy operator Σ is given in terms of quantities defined in (2) as

$$\Sigma(r_1,r_3,\omega)=\sqrt{\rho_0(r_1)\rho_0(r_3)}V(r_1-r_3) +\int\int\sqrt{\rho_0(r_1)\rho_0(r_4)}V(r_1-r_4) \times G_n(r_5-r_4,\omega)\sqrt{\rho_0(r_5)\rho_0(r_3)} \times V(r_5-r_3)d^3r_4d^3r_5\ . \tag{5}$$

In deriving this equation, we have specifically allowed for the spatial variation of the condensate density $\rho_0(r)$. Together Eqs. (4) and (5) contain all the dynamical information necessary to solve for the evaporation probabilities. Unfortunately, a direct solution of this system of equations is complicated by two features. First, Eq. (4) contains a *nonlocal* potential term, and second, Eq. (5) contains the propagator G_n. An exact solution to the equations must be self-consistent, and any attempt to iterate toward a stable solution is fraught with numerical difficulties.[27] Hence we must try to solve the equations in a more intuitive fashion.

If the surface width is large compared with the helium-helium interaction range (i.e., the atomic radius), the slow variation of the condensate density allows the use of a local-density approximation. Consider the terms in Eq. (5). The Green's function G_n is of very short range for all of the energies considered here (it varies as $e^{-\sqrt{2m\mu}|r_5-r_4|}$). The self-energy therefore can be written as

$$\Sigma(r_1,r_2,\omega)=\rho(r_1)V(r_1-r_3) +\rho^2(r_1)\int\int V(r_1-r_4)\tilde{G}_n(r_5-r_4,-\omega) \times V(r_5-r_3)d^3r_4d^3r_5\ , \tag{6}$$

where $\tilde{G}_n$ is evaluated at the density $\rho(r_1)$. Inserting the expression (6) into Eq. (4) gives the "local"-density equation. It is important to note that the nonlocality of the interaction has been retained in order to preserve the essential condensate properties. An approximate solution to the local-density equation can be found by using the WKB formalism.[28] The trial wave function is of the form

$$\varphi(x)=\frac{1}{\sqrt{k(x)}}\exp\left[\int_{-\infty}^{x}k(x')dx'\right]\ ,$$

where $k(x)$ is the wave vector of the quasiparticle in a homogeneous fluid of the density at x. Because of the nonlocality, there will be more than one value of k and it is important to follow the developing solution through the surface. Figure 4 shows how the energy spectrum changes as the density is decreased. The variation of the wave vector $k(x)$ with a given incident value enables four distinct WKB states to be constructed for each energy.

Consider the energy range between the roton minimum

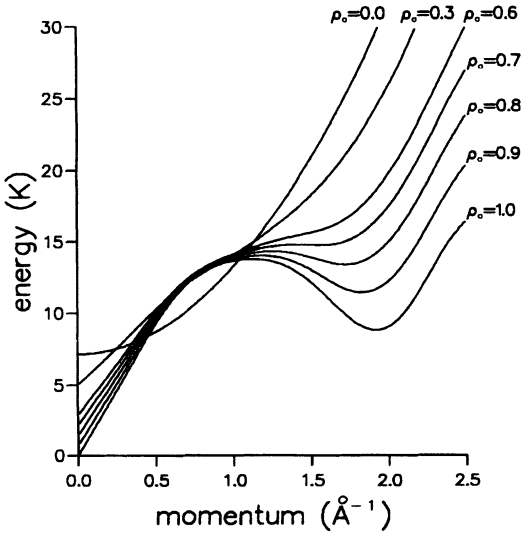

FIG. 4. Variation of Bogoliubov's spectrum with condensate density. $\rho_0=1.0$ corresponds to the bulk liquid, whereas $\rho_0=0.0$ is the free-atom spectrum of the vapor.

and the maxon. The first WKB state arises from an incoming phonon. As it progresses through the surface, the wave vector changes slowly and the quasiparticle converts smoothly into a free atom in the vacuum. The second state arises from the reverse process: An incoming atom converts to a phonon propagating away from the surface with the wave vector again changing smoothly through the surface. The other two states concern the rotons which, in the local-density limit, are trapped within the liquid. Consider an incident R^+ roton with energy below that of the maxon. As it moves into the surface, its wave vector drops rapidly to that of the minimum. Beyond this point its wave vector becomes complex, so that the energy is conserved throughout. Hence the roton wave function decays into the surface so that no energy is transmitted through to the vacuum side and the roton is reflected as a liquid quasiparticle. At the classical turning point, where the wave vector first becomes complex, the reflection that requires no momentum transfer is that to the R^- roton with the same energy and this then is the mode that the roton couples to. The third type of WKB state therefore describes an R^+ roton reflecting as an R^-. Similarly, the fourth state describes the reverse process of an R^- reflecting as its R^+ partner. We note that since the roton wave vectors are nonzero throughout, there is no difficulty in connecting these solutions. At energies above the maxon or below the roton minimum, the same calculations produce two states which propagate through the whole system, which correspond to evaporation of and condensation into R^+ rotons or phonons, respectively. The roton-minimum- and maxon-derived states are completely localized in the surface region and cannot carry any flux.

The results of the above analysis for the quantum-evaporation process are therefore that (a) phonons and high-energy R^+ rotons produce quantum evaporation with essentially unit probability, (b) helium atoms are absorbed with unit probability, and (c) R^+ and R^- rotons do not contribute to the evaporation process in the energy range between the roton minimum and the maxon. Although (a) and (b) are in qualitative agreement with experiment, (c) is clearly incorrect.

C. Coupling between the local-density WKB states

The current estimate of the width of the surface region of the superfluid is ~ 10 Å,[29] whereas the radius of the helium atoms is ~ 2.25 Å. It is therefore not surprising that the local-density solutions outlined above do not satisfactorily describe the real system. It is apparent that when the density variation is of the order of the quasiparticle wavelengths, the solutions of Eq. (4) must involve mixing between the quasiparticle modes. In order to estimate this mixing, we apply perturbation theory using the WKB states as a basis. The justification for such an approach is as follows. The WKB states are exact solutions to Eq. (4) deep in the liquid and also above the surface in the vacuum, where the density is constant. The only region where they are approximations is in the surface itself. Thus the exact Hamiltonian acts as a perturbative potential only at the surface, which then causes the transition of the quasiparticles from one WKB state to another. Because we are starting with solutions that are reasonable throughout and because the scattering only occurs in a small region of space, we can expect perturbation theory to yield acceptable results.

As a result of these considerations, we find the perturbing potential $U(r)$ defined through

$$U(r_1)\varphi(r_1)=\int \Sigma(r_1-r_3)\varphi(r_3)d^3r_3 - \int \Sigma_{\text{local}}(r_1-r_3)\varphi(r_3)d^3r_3$$

and the relevant matrix elements, for the scattering,

$$M_{ij}=\int \varphi_j(r)U(r)\varphi_i^*(r)d^3r \ ,$$

where $\varphi_i(r)$ are the WKB states. From this we calculate the various transition probabilities between the WKB states to be

$$P_{qq}=\frac{1}{N^2} \quad \text{and} \quad P_{qk}=\frac{|M_{qk}|^2}{N^2 v_g(q)v_g(k)} \ ,$$

where $v_g(q)$ is the group velocity of the state q and

$$P_{qq}+\sum_k P_{qk}=1$$

sets the value of the normalization constant N.

The expressions for the transition probabilities have been evaluated for atoms and quasiparticles impinging upon the surface in the normal direction. The experimentally measured quasiparticle-energy spectrum was used in the first instance to construct the four WKB states, utilizing the density dependence of Bogoliubov's formula (as in Fig. 4). The matrix elements between these states, M_{ij}, were calculated using the Brueckner pseudopotential,[26] which reduces the order of the numerical integrations to 3 for the case of normal incidence studied here. The self-energy [Eq. (5)] was evaluated using the local-density approximation for the denominator of the Green's function G_n as this is sufficient to give the leading-order dependence of Σ on the nonlocality of the interaction. We have used a Fermi-function for the surface profile, taking 10%-90% widths to be 5, 10, and 15 Å; although the middle value appears to best describe the system,[29] it is important to see how sensitive the results are to this parameter. The results of these calculations are presented below.

III. RESULTS

A. Incident atoms

In Fig. 5 we plot the various possible transition probabilities for atoms impinging upon the surface as a function of the energy of the incoming particles. Atoms at the lower end of the scale couple to phonons with energy just above the chemical potential, 7.16 K. The labels on the graphs correspond to those in Fig. 1, which indicate the momentum change required for each individual transition. The curves clearly show the division between the energy regimes. Atoms with energy above 6.6 K can couple to R^+ rotons, which are the only bulk quasiparticle

states with energy above the maxon. Thus the $A_i \rightarrow R_0^+$ transition probability increases suddenly at this value because this coupling is now the dominant WKB solution. The $A_i \rightarrow A_0$ atomic-reflectivity curves show discontinuities at this energy for surface widths 5 and 15 Å, but not for the 10-Å width, which presumably results from some interference effect. For atoms below 6.6 K, energy transitions to the other bulk modes are possible and the WKB solution is now $A_i \rightarrow P_0$ condensation. It can be seen that the $A_i \rightarrow A_0$ reflection can be quite high and so shows a significant difference to the WKB scenario. The reason for this is that the matrix element for this transition becomes large for low-energy atoms because both the incident-atom and incident-phonon WKB states are traveling waves and consequently have large overlap integrals. Low-energy atoms then show a strong reflection

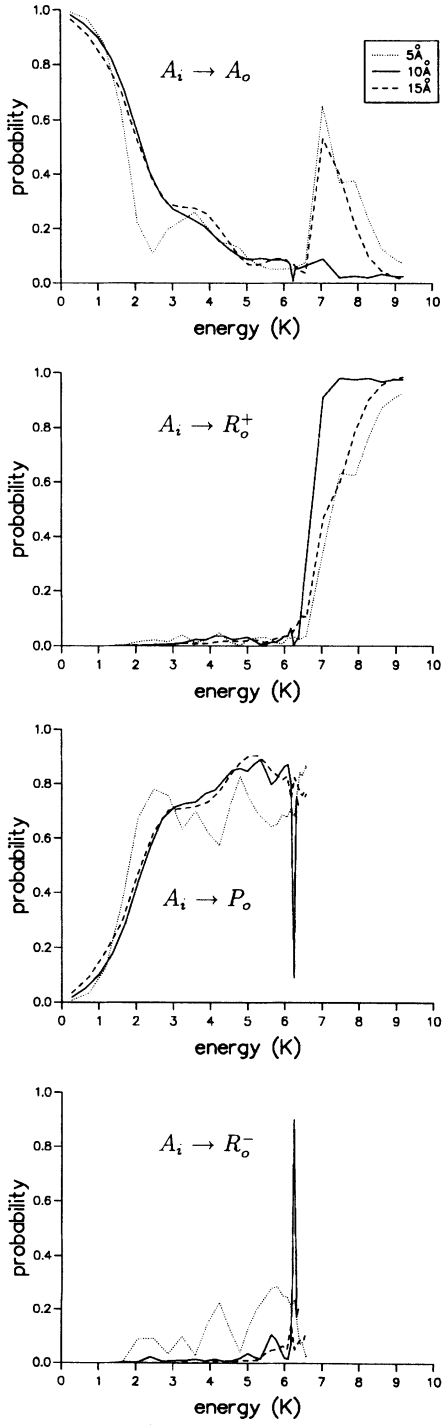

FIG. 5. Transition probabilities for incident atoms as a function of their energy in the vapor.

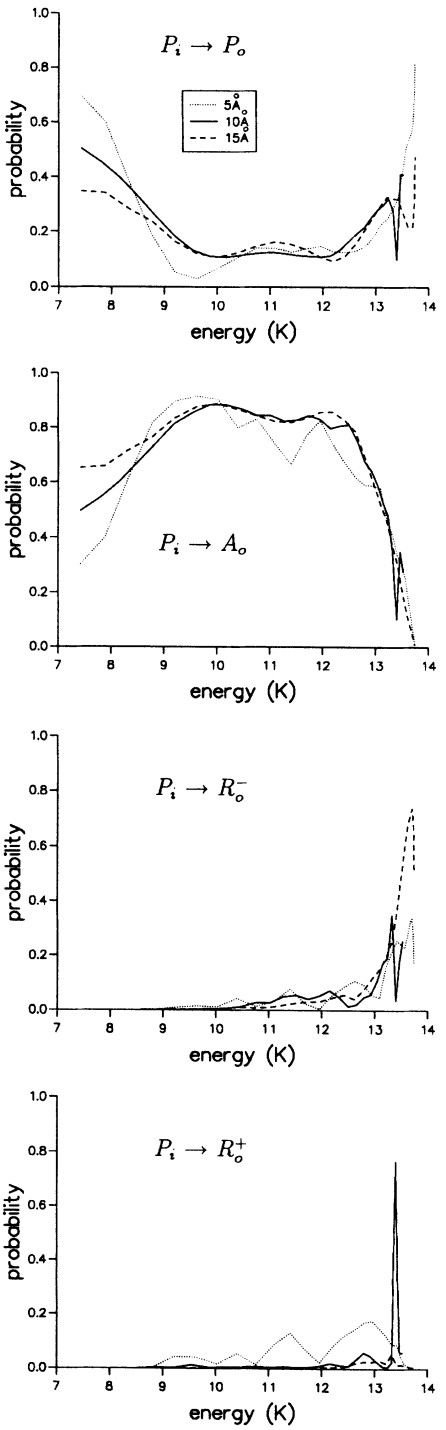

FIG. 6. Transition probabilities for incident phonons as a function of their energy in the liquid.

coefficient in agreement with basic wave-mechanical scattering theory, the probability for reflection rising to unity as the energy approaches zero. The coupling of low-energy atoms to the roton states is small because of the inherent difference between the traveling-wave atom or phonon WKB state and standing-wave R^+ or R^- states. The only exception occurs just below the maxon energy where the density of final states for R^- rotons diverges, causing a slight rise in the $A_i \rightarrow R_0^-$ transition probability. It is notable that the atomic-reflectivity curves do not show any discontinuity at the roton minimum threshold of 1.6 K because of the very small probabilities of condensation as rotons. This agrees with experimental observations.[15] The actual surface width has little effect on these results apart from the fact that the 5-Å curves tend to be little noisier. This can be attributed to the fact the WKB solutions are poor starting states for such a narrow surface.

B. Incident phonons

The transition probabilities for incident phonons are given in Fig. 6. Here the energy axis refers to the incoming excitations, so that only those above 7.16 K can couple to the atoms. The "WKB" channel, which is the evaporation of atoms, is found to dominate over most of the energy range. The reflection back from the surface into the phonon mode causes the largest reduction of the evaporation channel, which once again is due to the large matrix element between the two traveling-wave WKB states. It is interesting to note that the $P_i \rightarrow P_0$ probability does not rise to unity as the energy of the incident phonon decreases to the chemical potential, but instead the $P_i \rightarrow A_0$ channel remains active throughout mainly because of the large density of final states for the low-energy atoms. Reflection into the phonon channel increases in the vicinity of the maxon energy, as a result of the increasing density of final phonon states. Phonons do not couple strongly to the roton modes, again as a result of the essential mismatch between the WKB phonon and roton states in the surface regions which produce small matrix elements. Thus the phonon-evaporation curves do not show any discontinuities at the roton minimum threshold just as we found with the atomic reflectivity. The $P_i \rightarrow R_0^-$ probability does rise a little at the top end of the phonon-energy scale because of the diverging density of final R^- roton states and the convergence in character of the two modes at the maxon. (The 10-Å curve for the $P_i \rightarrow R_0^+$ does show a spike right at the maxon energy, but this feature is most probably caused by convergence problems with the numerical evaluation of the matrix element. Otherwise, the transition to the R^+ rotons is completely negligible.) Again, we observe that the surface width does not markedly affect the results for the phonon transitions.

C. Incident R^- rotons

The curves in Fig. 7 give the transition probabilities for incident R^- quasiparticles as a function of their energy in the liquid; the energy range on the x axis is from the roton minimum to the maxon energy. The WKB mode for these excitations is reflection as R^+ rotons. From the curves of $R_i^- \rightarrow R_0^+$, we see that the surface width has a much more marked effect on these results because of the fact the WKB states arise from a local-density consideration which is more appropriate for thick surfaces. The depletion of the WKB channel is caused mainly by the

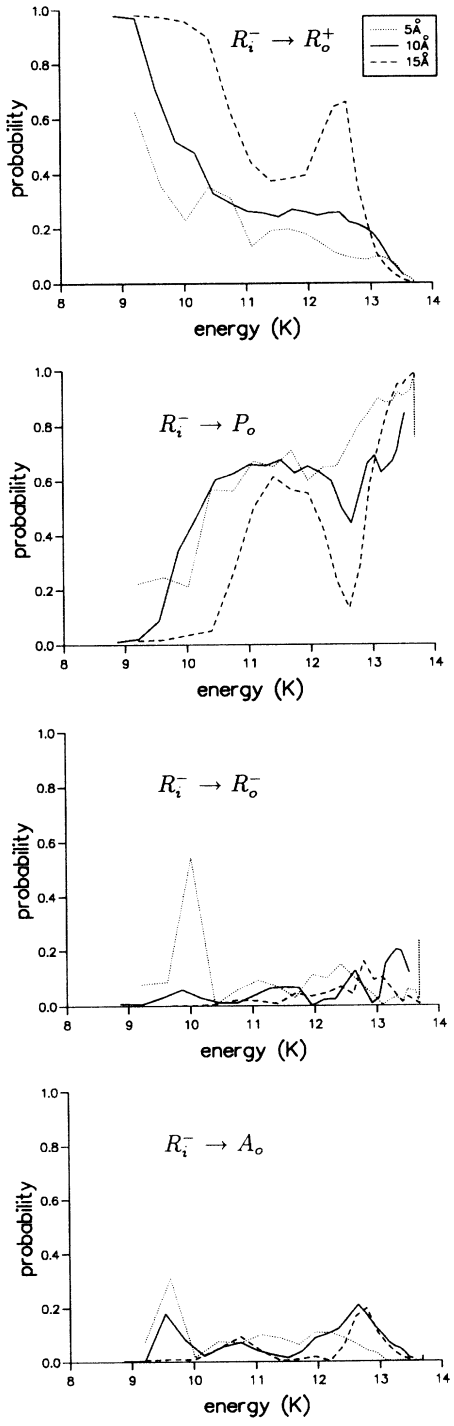

FIG. 7. Transition probabilities for incident R^- rotons as a function of their energy in the liquid.

transitions to reflected phonons, $R_i^- \rightarrow P_0$, the probability for which rises as the energy increases. There are two reasons for this behavior. First, the density of final phonon states increases with energy, and second, the matrix element for the transition also increases as the rotons gain more penetration of the surface. Similarly, the transition $R_i^- \rightarrow A_0$ also becomes possible as the rotons propagate further into the surface, even though this evaporation does require large momentum changes. However, it remains small throughout the energy range because the perturbing potential is due to the nonlocality of the interatomic potential and so is inherently unlikely to have the large high-momentum Fourier components necessary for the transition. For the same reason, the $R_i^- \rightarrow R_0^-$ reflection is small throughout the energy range.

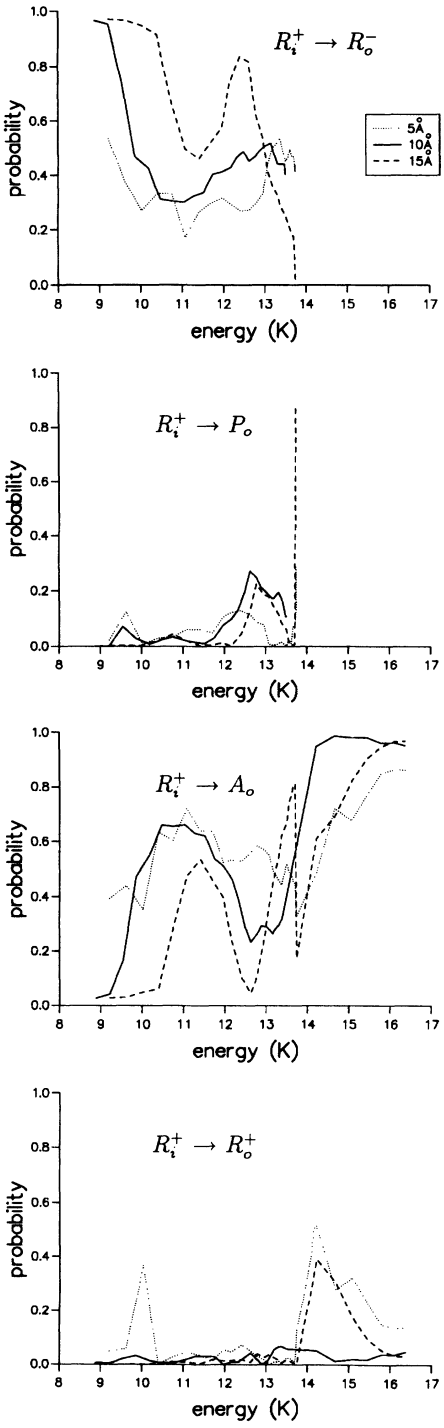

FIG. 8. Transition probabilities for incident R^+ rotons as a function of their energy in the liquid.

D. Incident R^+ rotons

Similar trends in the behavior of incident R^+ rotons are observed (see Fig. 8) in that the thicker surfaces show that the WKB channel of reflection as R^- largely dominates in the energy range from the minimum to the maxon. The $R_i^+ \rightarrow A_0$ transition becomes important as the energy increases again because of the rise in the overlap between the respective WKB states. The $R_i^+ \rightarrow P_0$ reflection, which requires large momentum changes, only becomes significant in the maxon region where the density of final phonon states is large. The curves $R_i^+ \rightarrow A_0$ and $R_i^+ \rightarrow R_0^+$ give the only possible transitions above the maxon energy. The evaporation is the dominant WKB solution in this energy regime, and the roton reflection dies away quickly as the energy increases beyond the maxon. Once again, we note that the 10-Å curve in the reflection passes smoothly through the maxon energy, in the same way as does the atomic reflectivity curve $A_i \rightarrow A_0$.

IV. DISCUSSION AND CONCLUSIONS

To summarize, the evaporation probability for phonons is high (~ 0.8) throughout the experimental energy range. Because of the coupling induced in the surface region, the low-energy R^+-roton-evaporation rate is now significant ($0.2 \rightarrow 0.6$), but the R^--roton-induced evaporation remains very small because of the large momentum change required. It is difficult to compare these figures with experimental values, because exact measurements of the probabilities have not in general been possible. However, the trends seen in experiments indicate that the probabilities should be numbers of the order of $0.1-1.0$.[20,30,31] This tends to support our results and contradicts the idea that ripplons seriously affect the atomic trajectories in the vapor.[16]

Wyborn and Wyatt[18] have performed some measurements of the evaporation of R^- rotons, which have been produced by condensing atoms. Unfortunately, in this experiment, the particles are all incident at an angle to the surface and the change in the normal component of the momentum required by the transitions is very much smaller than with the normal incidence; so the results are not comparable. Another experiment these authors performed[20] does lend support to our work. This experiment used mode changing at the free surface of $R^+ \rightarrow R^-$ rotons, and it was found that this transition has high probability, in agreement with the local-density WKB argument outlined here.

We now consider the atomic reflectivity, as given in Fig. 5, $A_i \rightarrow A_0$. Note that the general shapes of the

curves, with the reflectivity approaching unity as the energy goes to zero, are consistent with basic wave-mechanical scattering theory and comes from the mismatch in the group velocities. This does contradict the results of Edwards *et al.*,[15] who found that the reflectivity falls sharply as the atomic energy increases from zero. As they pointed out, this is probably due to an inelastic loss mechanism. However, as we have stated above, this mechanism is unlikely to be ripplon creation. The only other possibility is energy loss to a shower of low-energy phonons. This mechanism is feasible because the mean-free-path length for phonons below ~ 10 K is only ~ 100 Å in the bulk system[19] because of the three-phonon decay process. In the surface region, we can expect this length to be even smaller because more decay channels are possible since only the parallel component of momentum need be conserved. It would certainly appear to be possible for incident atoms below ~ 3 K energy to thus end up as shower of low-energy phonons in the liquid; the reflectivity of the atoms in this energy region would then be pulled drastically down by this inelastic mechanism, in line with the experimental results. However, this is just a speculative argument and the detailed calculations remain to be done.

In conclusion, then, we have successfully shown how one can adapt Beliaev's microscopic theory of superfluid ^{4}He to the quantum-evaporation phenomenon. The results of the analysis are found to be in broad agreement with experimental evidence. On the theoretical side, there is still much work to be done. The techniques developed here can be most easily adapted to the oblique scatterings of particles impinging upon a free surface. Similar calculations with solid surfaces will provide valuable insight to the workings of the heaters and bolometers used in experiments. Finally, the question of the production of low-energy phonons from atom condensation should be addressed to ascertain whether it is indeed the inelastic mechanism causing the high atomic absorption.

[1] P. L. Kapitza, Nature **141**, 74 (1932).
[2] L. D. Landau, J. Phys. (Moscow) **5**, 71 (1941).
[3] H. Palevsky, K. Otnes, and K. E. Larsson, Phys. Rev. **112**, 11 (1958).
[4] W. D. Johnston, Jr. and J. G. King, Phys. Rev. Lett. **16**, 119 (1966).
[5] S. Balibar, J. Buechner, B. Castaing, C. Laroche, and A. Libchaber, Phys. Rev. B **18**, 3096 (1978).
[6] M. J. Baird, F. R. Hope, and A. F. G. Wyatt, Nature **304**, 325 (1983).
[7] A. F. G. Wyatt, Physica **126B**, 392 (1984).
[8] M. Brown and A. F. G. Wyatt, J. Phys. Condens. Matter **2**, 5025 (1990).
[9] G. M. Wyborn and A. F. G. Wyatt, Jpn. J. Appl. Phys. Suppl. **26**, 2095 (1987).
[10] A. F. G. Wyatt, in *Phonons 89*, edited by S. Hunklinger, W. Ludwig, and G. Weiss (World Scientific, Singapore, 1990), p. 1019.
[11] P. W. Anderson, Phys. Lett. **29A**, 563 (1969).
[12] D. S. Hyman, M. O. Scully, and A. Widom, Phys. Rev. **186**, 231 (1969).
[13] J. G. King, J. McWane, and R. Tinker, Bull. Am. Phys. Soc. **17**, 38 (1972).
[14] M. W. Cole, Phys. Rev. Lett. **28**, 1622 (1972).
[15] D. O. Edwards, P. P. Fatouros, G. G. Ihas, P. M. Rozinsky, S. Y. Shen, F. M. Gasparini, and C. P. Tam, Phys. Rev. Lett. **34**, 1153 (1975).
[16] P. M. Echenique and J. B. Pendry, Phys. Rev. Lett. **37**, 561 (1976); J. Phys. C **9**, 3183 (1976).
[17] D. O. Edwards, G. G. Ihas, and C. P. Tam, Phys. Rev. B **16**, 3122 (1977).
[18] G. M. Wyborn and A. F. G. Wyatt, Phys. Rev. Lett. **65**, 345 (1990).
[19] H. J. Maris, Rev. Mod. Phys. **49**, 341 (1977).
[20] G. M. Wyborn, Ph.D. thesis, Exeter University, 1989.
[21] A. Griffin, Phys. Lett. **31A**, 222 (1970).
[22] S. T. Beliaev, Zh. Eksp. Teor. Fiz. **34**, 417 (1958) [Sov. Phys. JETP **7**, 289 (1958)].
[23] L. Tisza, Nature **171**, 913 (1938).
[24] E. C. Svensson, in *Proceedings of the 75th Jubilee Conference on Helium-4*, edited by J. G. Armitage (World Scientific, Singapore, 1983), p. 10.
[25] N. Bogoliubov, J. Phys. (Moscow) **11**, 23 (1947).
[26] K. A. Brueckner and K. Sawada, Phys. Rev. **106**, 1117 (1957).
[27] P. A. Mulheran, Ph.D. thesis, Exeter University, 1991.
[28] See, for example, L. I. Schiff, *Quantum Mechanics*, 3rd ed. (McGraw-Hill, New York, 1981), p. 269.
[29] D. V. Osbourne, J. Phys. Condens. Matter **1**, 289 (1989).
[30] P. Fozooni, D. S. Spencer, and M. J. Lea, Jpn. J. Appl. Phys. Suppl. **26**, 281 (1987).
[31] S. Mukherjee, D. O. Edwards, and S. Kumar (unpublished).